Benchmarking the performance of spin-component scaled CC2 in ground and electronically excited states

Arnim Hellweg,† Sarah A. Grün and Christof Hättig*

Received 4th March 2008, Accepted 15th April 2008
First published as an Advance Article on the web 5th June 2008
DOI: 10.1039/b803727b

A generalization of the spin-component scaling and scaled opposite-spin modifications of second-order Møller–Plesset perturbation theory to the approximate coupled-cluster singles-and-doubles model CC2 (termed SCS-CC2 and SOS-CC2) is discussed and a preliminary implementation of ground and excited state energies and analytic gradients is reported. The computational results for bond distances, harmonic frequencies, adiabatic and 0–0 excitation energies are compared with experimental results to benchmark their performance. It is found that both variants of the spin-scaling increase the robustness of CC2 against strong correlation effects and lead for this method even to somewhat larger improvements than those observed for second-order Møller–Plesset perturbation theory. The spin-component scaling also enhances systematically the accuracy of CC2 for 0–0 excitation energies for $\pi \rightarrow \pi^*$ and $n \rightarrow \pi^*$ transitions, if geometries are determined at the same level.

I. Introduction

Quantum chemistry is always a compromise between accuracy and computational costs. Highly accurate methods are generally too demanding to be used for large systems, while economical methods are often based on crude approximations that restrict their applicability. This simple observation already outlines an important objective of quantum chemistry: to spot ways of implementing existing ansätze more efficiently or ways to increase the accuracy of economical methods *via* an improved description of the underlying physics. In summary, this means that quantum chemical approaches have to become faster or more accurate or both.

Coupled-cluster linear response theory, which is the theoretical basis and the numerical framework of the presented approaches, provides a systematic route to approach the full CI limit for single-reference ground state and electronically excited state calculations. With the inclusion of connected multiple excitations in the wavefunction within the hierarchy of truncated coupled-cluster methods CCS, CCSD, CCSDT, ...the accuracy is improved fast and systematically. However also the computational costs increase very soon as is evident from their formal scaling with the system size $\mathcal{N}$ as, respectively, $\mathcal{O}(\mathcal{N}^4)$, $\mathcal{O}(\mathcal{N}^6)$, and $\mathcal{O}(\mathcal{N}^8)$. Intermediate methods, based on the perturbation theory, can be inserted in this hierarchy as, *e.g.*, second-order Møller–Plesset perturbation theory, MP2, ($\mathcal{O}(\mathcal{N}^5)$) and CCSD with a perturbative correction for connected triples, CCSD(T), ($\mathcal{O}(\mathcal{N}^7)$) for ground-state calculations or CC2 ($\mathcal{O}(\mathcal{N}^5)$) and CC3 ($\mathcal{O}(\mathcal{N}^7)$) for linear response calculations. With the inclusion of connected triple excitations usually chemical accuracy is reached. CCSD(T) can today be regarded as a kind of gold standard in computational chemistry for ground-state calculations. The inclusion of double excitations, at least at the level of MP2 or CC2, is indispensable for the description of dynamic electron–electron correlation.

Density functional theory (DFT) offers a back door to dynamic correlation at low computational costs. DFT scales formally with $\mathcal{O}(\mathcal{N}^4)$ for hybrid functionals, but—in particular for pure density functionals—most implementations realize lower scalings with $\mathcal{O}(\mathcal{N}^3) - \mathcal{O}(\mathcal{N}^2)$ to an almost linear scaling by integral screening, resolution-of-the-identity and fast multipole methods (FMM). In many cases DFT achieves a similar accuracy as second-order methods. Electronically excited states are in DFT—similar as for coupled-cluster methods—accessed through linear response theory, which leads to TDDFT. However despite its great success for ground-state calculations, with contemporary functionals DFT still has severe technically problems in the description of charge transfer states, dispersive interactions, and Rydberg excitations.

Recently Grimme *et al.*[1,2] proposed for MP2 an empirical scaling of the energy contributions of the same- and opposite-spin components (*i.e.* essentially of the coulomb and exchange correlation contributions), SCS-MP2, which significantly improves the performance of MP2 for many applications at no additional computational costs. An attempt to use the SCS-MP2 wavefunction to improve the performance of the perturbative doubles correction for configuration interaction singles, CIS(D), has also been reported,[3] but the results have not been conclusive. Head-Gordon *et al.*[4–7] showed that with an appropriate scaling of the opposite-spin component it is even possible to abandon completely the same-spin or exchange correlation contribution without significant loss in accuracy. With resolution-of-the-identity techniques, the so-called SOS versions of MP2 and CIS(D) can be implemented with a formal $\mathcal{O}(\mathcal{N}^4)$-scaling of the computational costs, *i.e.*

Lehrstuhl für Theoretische Chemie, Ruhr-Universität Bochum, D-44780 Bochum, Germany.
E-mail: christof.haettig@theochem.rub.de
† Present address: COSMOlogic GmbH & Co. KG, Burscheider Strasse 515, D-51381 Leverkusen, Germany.

with similar costs as Hartree–Fock or DFT with hybrid functionals.

In the present paper we investigated the performance of the SCS and SOS scalings for the approximate coupled-cluster singles-and-doubles model CC2. This model can be understood as a generalization of MP2 with an iterative treatment of single excitations. This allows to apply the framework of coupled-cluster response theory to this second-order method to calculate excitation energies, transition properties as well as structures and properties of excited states. As it is not based on non-degenerate perturbation theory, it does not suffer from the shortcomings[8] of CIS(D) in the calculation of potential energy surfaces. It has in recent years been successfully applied for the investigation of excited state structures of several medium-sized molecules[9–11] and developed to an important alternative to TDDFT in the study of charge-transfer states.[12–14] A problem of CC2 is its (compared to MP2) enhanced sensitivity to strong correlation effects in the ground state caused by the inclusion of single excitations in the ground-state wavefunction.[15] As we will show in the present work, the damping of the exchange correlation contribution to the wavefunction by a scaling of the spin-components of the double excitations recovers a more balanced account of the correlation effects. And, of course, a reduction of the scaling of its computational costs—formally from $\mathcal{O}(\mathcal{N}^5)$ to $\mathcal{O}(\mathcal{N}^4)$—with an SOS-like modification would greatly improve its applicability to larger systems.

II. Theory

A Spin-component scaled MP2

The spin-component scaled MP2 approach was defined by Grimme in ref. 1 by introducing independent empirical scaling factors for the same and opposite spin contributions to the MP2 correlation energy:

$$E_{\mathrm{SCS-MP2}} = E_{\mathrm{SCF}} + \frac{1}{2}\sum_{\sigma\sigma'} c_{\sigma\sigma'} \sum_{iajb} t_{ia,jb}^{\sigma\sigma'} [(ia\sigma|jb\sigma') - \delta_{\sigma\sigma'}(ib\sigma|ja\sigma)]. \quad (2.1)$$

In the latter equation $t_{ia,jb}^{\sigma'}$ are the double excitation amplitudes of the first-order wavefunction

$$t_{ia,jb}^{\sigma,\sigma'} = \frac{(ia\sigma|jb\sigma')}{\varepsilon_i^\sigma - \varepsilon_a^\sigma + \varepsilon_j^{\sigma'} - \varepsilon_b^{\sigma'}} \quad (2.2)$$

and we used the convention that i, j and a, b denote, respectively, occupied and virtual orbitals and σ and σ' indicate the spin case (α or β). The coefficients $c_{\alpha\alpha} = c_{\beta\beta} = c_{\mathrm{SS}}$ and $c_{\alpha\beta} = c_{\alpha\beta} = c_{\mathrm{OS}}$ are the scaling factors for the energy contributions from the same (SS) and the opposite (OS) spin components of the first-order wavefunction. If c_{SS} is set to zero and c_{OS} to 1.3 one obtains the spin-opposite scaled (SOS) approximation proposed by Jung *et al.*[4] To have a compact notation for the generalization to the approximate coupled-cluster model CC2, we introduce the double excitation operators

$$\hat{T}_2^{\sigma\sigma'} = \sum_{iajb} t_{ia,jb}^{\sigma,\sigma'} \hat{\tau}_{ai}^{\sigma} \hat{\tau}_{bi}^{\sigma'} \text{ with } \hat{\tau}_{ai}^{\sigma} = \hat{a}_{a\sigma}^{\dagger} \hat{a}_{i\sigma}, \quad (2.3)$$

where $\hat{a}_{a\sigma}^{\dagger}$ and $\hat{a}_{i\sigma}$ are the usual creation and annihilation operators in the second quantization formalism. With these operators the expression for a spin-component scaled MP2 energy can be written as:

$$E_{\mathrm{SCS-MP2}} = \langle \mathrm{HF}|\hat{H} + \sum_{\sigma\sigma'} c_{\sigma\sigma'} [\hat{H}, \hat{T}_2^{\sigma\sigma'}]|\mathrm{HF}\rangle \quad (2.4)$$

with the amplitudes in $\hat{T}_2^{\sigma\sigma'}$ determined by the condition

$$0 = \langle \mu_2^{\sigma,\sigma'}|[\hat{F}, T_2^{\sigma,\sigma'}] + \hat{H}|\mathrm{HF}\rangle. \quad (2.5)$$

In the last equation $\langle \mu_2^{\sigma,\sigma'}|$ is the doubles projection manifold[16] which is chosen biorthogonal to the determinants $\hat{\tau}_{ai}^{\sigma}\hat{\tau}_{bj}^{\sigma'}|\mathrm{HF}\rangle$. Eqn (2.5) suggests to interpret the spin-component scaling as an empirical correction or approximation to the first-order wavefunction. However note that the scaling can alternatively be incorporated partially or completely into the fluctuation potential $\hat{\phi} = \hat{H} - \hat{F}$ if the latter is split into different spin components. This would relate the SCS-MP2 and SOS-MP2 models to modified perturbation expansions, which might provide a possible route for generalizations to higher-order. Here, we will not pursue this idea further as our aim is to investigate a generalization of the spin-component scaling to the second-order coupled-cluster model CC2 and its application within the framework of coupled-cluster response theory.

B Generalization to the CC2 model

The approximate coupled-cluster singles-and-doubles model CC2 is defined by the energy expression and the equations for the singles and the doubles cluster amplitudes. MP2 can be obtained from CC2 by setting the singles amplitudes to zero, as the expression for the energy and the equations for the doubles amplitudes for CC2 differ from those for MP2 only by a replacement of $\hat{H}$ by the $\hat{T}_1$-similarity transformed Hamiltonian $\tilde{\hat{H}} = \exp(-\hat{T}_1)\hat{H}\exp(\hat{T})$. We keep this connection for the spin-component scaled versions and introduce the scaling in these equations as:

$$E_{\mathrm{SCS-CC2}} = \langle \mathrm{HF}|\tilde{\hat{H}} + \sum_{\sigma\sigma'} c_{\sigma\sigma'} [\tilde{\hat{H}}, \hat{T}_2^{\sigma\sigma'}]|\mathrm{HF}\rangle, \quad (2.6)$$

$$\langle \mu_2^{\sigma,\sigma'}|[\hat{F}, \hat{T}_2^{\sigma,\sigma'}] + \tilde{\hat{H}}|\mathrm{HF}\rangle = 0, \quad (2.7)$$

In addition, we must specify the equations for the singles amplitudes. A natural choice is to apply the spin-component scaling to the second-order term in these equations $[\hat{H}, \hat{T}_2]$ in the same way as in the energy expression:

$$\langle \mu_1|\tilde{\hat{H}} + \sum_{\sigma,\sigma'} c_{\sigma,\sigma'} [\tilde{\hat{H}}, \hat{T}_2^{\sigma,\sigma'}]|\mathrm{HF}\rangle = 0. \quad (2.8)$$

The single excitations contribute to the ground state energy first in fourth order in the fluctuation potential. Therefore, the precise form in which the spin-component scaling is introduced in the last equation is expected to have little effect on the ground state potential energy surface. The singles play, however, a crucial role in the calculation of excitation energies and properties within the framework of coupled-cluster response theory. The interplay between the second-order term in eqn (2.8) and $\hat{H}$ in eqn (2.7) determines the differential dynamic correlation between the ground and excited states.

This journal is © the Owner Societies 2008

Vertical excitation energies are obtained as eigenvalues of the Jacobi matrix which contains as elements the derivatives of the left sides of eqns (2.8) and (2.7) with respect to the cluster amplitudes:

$$\boldsymbol{A} = \begin{pmatrix} \boldsymbol{A}_{\mu_1\nu_1} & \boldsymbol{A}_{\mu_1\nu_2} \\ \boldsymbol{A}_{\mu_2\nu_1} & \boldsymbol{A}_{\mu_2\nu_2} \end{pmatrix} = \left(\begin{array}{c|c} \langle \mu_1 | \left[(\tilde{\hat{H}} + \sum_{\sigma\sigma'} c_{\sigma\sigma'} [\tilde{\hat{H}}, T_2^{\sigma\sigma'}]), \hat{\tau}_{\nu_1} \right] | \mathrm{HF} \rangle & \langle \mu_1 | c_{\sigma\sigma'} [\tilde{\hat{H}}, \tau_{\nu_2}^{\sigma\sigma'}] | \mathrm{HF} \rangle \\ \hline \langle \mu_2^{\sigma\sigma'} | [\tilde{\hat{H}}, \tau_{\nu_1}] | \mathrm{HF} \rangle & \langle \mu_2^{\sigma\sigma'} | [F, \tau_2^{\sigma\sigma'}] | \mathrm{HF} \rangle \end{array} \right). \tag{2.9}$$

With canonical molecular orbitals the doubles/doubles block $\boldsymbol{A}_{\mu_2\nu_2}$ is diagonal with the diagonal elements equal to the orbital energy differences $\varepsilon_a - \varepsilon_i + \varepsilon_b - \varepsilon_j = \varepsilon_{aibj}$. This allows to partition the CC2 eigenvalue problem

$$\begin{pmatrix} \boldsymbol{A}_{\mu_1\nu_1} & \boldsymbol{A}_{\mu_1\nu_2} \\ \boldsymbol{A}_{\mu_2\nu_2} & \delta_{\mu_2\nu_2}\varepsilon_{\mu_2} \end{pmatrix} \begin{pmatrix} \boldsymbol{E}_{\nu_1} \\ \boldsymbol{E}_{\nu_2} \end{pmatrix} = \omega \begin{pmatrix} \boldsymbol{E}_{\nu_1} \\ \boldsymbol{E}_{\nu_2} \end{pmatrix}, \tag{2.10}$$

for singles excitations to a nonlinear eigenvalue problem in the space of only the singly excited determinants, which plays a key role in making CC2 applicable to large systems:

$$\left[\boldsymbol{A}_{\mu_1\nu_1} - \sum_{\mu_2} \frac{\boldsymbol{A}_{\mu_1\mu_2}\boldsymbol{A}_{\mu_2\nu_1}}{\varepsilon_{\mu_2} - \omega} \right] \boldsymbol{E}_{\nu_1} = \omega \boldsymbol{E}_{\mu_1}. \tag{2.11}$$

If we split $\boldsymbol{A}_{\mu_1\nu_1}$ into the terms $\boldsymbol{A}_{\mu_1\nu_1}{}^{(0)}$ and $\boldsymbol{A}_{\mu_1\nu_1}{}^{(2)}(\hat{T}_2)$ which arise, respectively, from the contributions of $\tilde{\hat{H}}$ and $[\tilde{\hat{H}}, \hat{T}_2]$ in the singles eqn (2.8), the effect of the spin-component scaling in the CC2 eigenvalue problem can be expressed as:

$$\left[\boldsymbol{A}_{\mu_1\nu_1}^{(0),ns} + \sum_{\sigma,\sigma'} c_{\sigma\sigma'} \left\{ \boldsymbol{A}_{\mu_1\nu_1}^{(2),ns}(\hat{T}_2^{\sigma,\sigma'}) - \sum_{\mu_2} \frac{\boldsymbol{A}_{\mu_1\mu_2}^{ns,\sigma\sigma'}\boldsymbol{A}_{\mu_2\nu_1}^{ns,\sigma\sigma'}}{\varepsilon_{\mu_2} - \omega} \right\} \right]$$
$$E_{\nu_1} = \omega E_{\mu_1}. \tag{2.12}$$

The upper index *ns* indicates that expressions are given in terms of the un-scaled matrices. In the last equation the first term in the curled braces accounts in the Jacobian or response matrix for correlation effects from the ground state wavefunction while the second term accounts for the double excitation contributions to the eigenvector, which describes the excitation process from the correlated ground state to the excited state. By straightforward application of response theory to the spin-scaled CC2 models defined through eqns (2.6) and (2.7) we obtain for both contributions the same scaling factors. This restriction could be lifted by introducing in eqn (2.12) additional parameters which could be tuned to improve the performance of these approaches. Indeed the SCS-CIS(D) and SOS-CIS(D) models proposed recently by Grimme and Ugorodina[3] and Rhee and Head-Gordon[7] can be derived from the generalized response matrix

$$\boldsymbol{A}_{\mu_1\nu_1}^{(0),ns} + \sum_{\sigma,\sigma'} c_{\sigma\sigma'}^{gs} \boldsymbol{A}_{\mu_1\nu_1}^{(2),ns}(\hat{T}_2^{\sigma,\sigma'}) - \sum_{\sigma,\sigma'} c_{\sigma\sigma'}^{ex} \sum_{\mu_2} \frac{\boldsymbol{A}_{\mu_1\mu_2}^{ns,\sigma\sigma'}\boldsymbol{A}_{\mu_2\nu_1}^{ns,\sigma\sigma'}}{\varepsilon_{\mu_2} - c_\omega \omega} \tag{2.13}$$

in the same way as (non-scaled) CIS(D) from the Jacobi matrix of standard CC2. We also note that by calculating the Jacobian from the MP2 instead of the CC2 singles and doubles amplitudes and symmetrizing the matrix $\boldsymbol{A}_{\mu_1\nu_1}{}^{(2),ns}(\hat{T}_2^{\sigma,\sigma'})$ one obtains[17] spin-scaled versions of the algebraic diagrammatic construction[18] through second-order, ADC(2). In the present investigation we refrained from such modifications as they break some useful connections obtained from the response theory framework.

III. Implementation and computational details

We have implemented the spin-component scaled CC2 models defined in the last section, eqns (2.6)–(2.8), for ground state and excitation energies and the respective analytic gradients for the potential energy surfaces in the RICC2 program[15,19,20] of the TURBOMOLE package.[21] This implementation employs the resolution-of-the-identity (RI) approximation[22,23] and a partitioned doubles-amplitude direct strategy to make the CC2 model applicable to large molecules.[19] Even though we gave in the last section for convenience all expressions in the spin–orbit formalism, the spin-component scaled CC2 models can, similarly as SCS-MP2 for closed-shell systems, be easily implemented in the spin-free formalism for both singlet and triplet excited states.

To explore the performance of the spin-component scaled CC2 variants we carried out calculations for a set of small di- and triatomic molecules (see Tables 1–3) and a collection of organic molecules taken from ref. 3 (see Tables 4 and 5). For the di- and triatomic molecules the reported results have been obtained with the correlation-consistent quadruple-ζ basis sets cc-pVQZ and cc-pV(Q + d)Z from ref. 24 and 25 for molecules containing only first- and second-row elements and with the QZVPP basis from ref. 26 for molecules containing also the third-row elements Ga–Br. The results listed in Table 4 have been obtained using ground and excited state structures and vibrational frequencies calculated with (TD)DFT/B3-LYP in the TZVP basis set[27,28] using the egrad[29] module of the TURBOMOLE package. The CC2 calculations for these molecules have been carried out in the aug-cc-pVTZ basis set. For the MP2 and CC2 calculations we used a development version of the RICC2 module of TURBOMOLE with the optimized auxiliary basis sets for the resolution of the identity reported in ref. 28, 30 and 31. For the calculations with the spin-component variants of CC2 we used for ground and excited states the standard scaling factors proposed in ref. 1 and 4 for MP2 (SCS: $c_{SS} = 1/3$, $c_{OS} = 6/5$; SOS: $c_{SS} = 0$, $c_{OS} = 1.3$).

IV. Ground state

Due to the iterative inclusion of the singles amplitudes in CC2 ground state geometries and vibrational frequencies show some typical differences to results obtained with MP2. Typically, at the CC2 level bond lengths are slightly longer, in particular if strong correlation effects are encountered as in triple bonds or bonds between atoms with several lone pairs as *e.g.* in F_2 or ClOH. As a consequence of this weakening of covalent bonds vibrational frequencies calculated with CC2

Table 1 Errors in ground state bond distances (r_e) for MP2 and CC2 and their spin-component scaled SCS and SOS versions (in pm) with respect to experimental reference values listed in the right-most column. The second and third columns lists the D_1 and D_2 diagnostics[32,33] for strong correlation effects evaluated with the CC2 wavefunction. At the end of the table the average (Av. Error, $[\sum_i(r_e^{\mathrm{calc}}(i) - r_e^{\mathrm{exp}}(i))]/n$), the mean absolute (MAE, $[\sum_i|r_e^{\mathrm{cal}}(i) - r_e^{\mathrm{exp}}(i)|]/n$), and maximum absolute error (Max. Abs., $\max(|r_e^{\mathrm{calc}}(i) - r_e^{\mathrm{exp}}(i)|)$), and the standard deviation (Std. Dev. $\sqrt{\sum_i(r_e^{\mathrm{calc}}(i) - r_e^{\mathrm{exp}}(i))^2/(N-1)}$) are given for the present test set. The experimental values were taken from ref. 35

			MP2			CC2			
	D_1(CC2)	D_2(CC2)	(un-scaled)	SCS	SOS	(un-scaled)	SCS	SOS	Exp.
H_2	0.01	0.10	−0.5	−0.4	−0.4	−0.5	−0.4	−0.4	74.1
NH	0.01	0.13	−0.7	−0.7	−0.7	−0.5	−0.5	−0.4	103.6
CH	0.01	0.13	−0.8	−0.8	−0.7	−0.7	−0.6	−0.6	112.0
BH	0.02	0.13	−0.7	−0.7	−0.7	−0.7	−0.6	−0.6	123.2
OH	0.02	0.13	−0.4	−0.4	−0.4	−0.2	−0.2	−0.2	97.0
HCl	0.01	0.14	−0.3	−0.2	−0.2	−0.3	−0.2	−0.1	127.5
HF	0.02	0.14	−0.0	−0.0	−0.0	+0.2	+0.2	+0.1	91.7
BCl	0.03	0.11	−0.5	−0.1	+0.1	−0.1	+0.2	+0.4	171.5
Br_2	0.02	0.15	−2.2	−0.6	+0.2	−1.9	−0.3	+0.5	228.1
Cl_2	0.02	0.20	−0.9	+0.2	+0.8	−0.7	+0.5	+1.1	198.8
N_2	0.03	0.23	+1.2	+0.9	+0.7	+2.0	+1.5	+1.2	109.8
BF	0.04	0.16	+0.1	+0.2	+0.2	+0.7	+0.6	+0.5	126.3
ClF	0.04	0.22	−0.3	+0.3	+0.6	+0.5	+1.1	+1.5	162.8
S_2	0.04	0.23	+0.4	−0.1	−0.3	+1.2	+0.5	+0.2	188.9
GaH	0.05	0.10	−2.3	−1.5	−1.2	−2.3	−1.5	−1.1	166.3
GaBr	0.05	0.11	−1.2	+0.2	+1.0	−1.4	+0.2	+1.0	235.2
GaF	0.05	0.16	−0.1	+0.3	+0.5	+0.7	+0.9	+1.0	177.4
CO	0.05	0.21	+0.7	+0.4	+0.3	+1.7	+1.2	+1.0	112.8
SiS	0.05	0.21	+0.7	+0.6	+0.5	+2.1	+1.7	+1.5	192.9
SO	0.05	0.25	+0.4	−0.5	−1.0	+2.1	+0.8	+0.2	148.1
F_2	0.03	0.27	−1.5	−0.4	+0.1	+0.2	+1.4	+2.2	141.2
O_2	0.05	0.27	+1.1	−0.1	−0.7	+3.2	+1.2	+0.4	120.8
P_2	0.04	0.26	+2.0	+1.5	+1.2	+3.3	+2.6	+2.2	189.3
B_2	0.05	0.32	+0.4	−0.3	−0.6	+1.2	+0.2	−0.2	159.0
AsF	0.06	0.19	+0.1	+0.3	+0.5	+1.1	+1.2	+1.2	173.6
CF	0.07	0.18	−0.2	−0.1	−0.0	+0.9	+0.8	+0.7	127.2
CS	0.07	0.24	+0.1	−0.0	−0.1	+2.1	+1.5	+1.3	153.5
SeO	0.07	0.28	−1.0	−2.1	−2.7	+1.6	−0.1	−0.7	164.8
GeS	0.08	0.16	−0.2	−0.0	+0.2	+1.7	+1.6	+1.5	201.2
BO	0.08	0.22	+0.3	−0.1	−0.3	+1.7	+1.4	+1.2	120.5
NF	0.09	0.19	−0.7	−0.3	−0.1	+0.8	+0.9	+1.0	131.7
SeC	0.09	0.19	−0.6	−0.6	−0.5	+2.5	+1.9	+1.6	167.6
SiO	0.09	0.25	+1.6	+1.2	+1.0	+4.1	+3.0	+2.5	151.0
C_2	0.09	0.41	+1.3	+0.9	+0.7	+3.3	+2.5	+2.1	124.3
Av. Error			−0.13	−0.09	−0.06	+0.87	+0.73	+0.70	
MAE			0.75	0.51	0.56	1.42	0.99	0.95	
Std. Dev.			0.96	0.70	0.76	1.53	1.01	0.93	
Max. Abs.			2.3	2.1	2.7	4.1	3.0	2.5	

are systematically somewhat lower than those obtained with MP2. In some cases this increases, in other cases it reduces the remaining errors of CC2 compared to MP2, but for well behaved molecules with the diagnostics[15,32,33] $D_1 \lesssim 0.07$ and $D_2 \lesssim 0.2$ the accuracy reached with CC2 for ground state geometries and vibrational frequencies is on average similar to the accuracy of MP2.

To investigate how a spin-component scaling changes the performance of the CC2 model for ground state geometries and vibrational frequencies, we used a test set of 34 diatomic molecules that contain H, first-, second-, and third-row main group elements and cover a range for D_1 up to 0.09 and for D_2 up to 0.41. The results obtained with CC2 and its SCS and SOS variants for the bond lengths are listed in Table 1 together with the results for the corresponding MP2 approaches. The changes in the bond lengths upon spin-component scaling are in most cases at the CC2 level in the same direction as for MP2, but are usually more emphasized: *e.g.* for N_2 the bond length reduces from CC2 to its SCS and SOS variants by 0.5 and 0.8 pm, respectively, compared to 0.3 and 0.5 pm for the corresponding MP2 approaches. For both, MP2 and CC2 we find that triple and double bonds are shortened by the spin-component scaling, while single bonds are elongated, in particular between atoms with several lone pairs as *e.g.* F_2, Cl_2, Br_2, and ClF. The latter molecules belong also to the few exceptions for which the spin-component scaling for CC2 increases the error in the bond lengths.

The effects of the spin-component scaling on the vibrational frequencies follow largely the changes in the bond lengths: for the bonds which become shorter (stronger) the vibrational frequencies increase from the unmodified to the SCS and the SOS variants of MP2 and CC2, while vibrational frequencies are scaled down for those bonds which become longer (weaker) upon spin-component scaling. A summary of the results for the ground state vibrational frequencies for the molecules used to benchmark the bond distances is depicted in Fig. 1.

 This journal is © the Owner Societies 2008

Table 2 Errors in excited state bond distances (r_e, in pm) for CC2 and its spin-component scaled SCS and SOS versions. For HCN and HCP, respectively, the CN and CP distances are listed; for the definition of the average, mean absolute and maximum error and the standard definition see Table 1. The experimental values of the diatomic molecules were taken from ref. 35, the values for triatomic molecules are from the compilation in ref. 20

		CC2	SCS-CC2	SOS-CC2	Exp.
BH	$1\,^1\Pi$	−1.1	−1.0	−0.9	121.9
BF	$1\,^1\Pi$	+1.7	+1.4	+1.4	130.4
BF	$1\,^3\Pi$	+1.4	+1.3	+1.2	130.8
N_2	$1\,^3\Pi_g$	+3.8	+2.8	+2.4	121.3
N_2	$1\,^1\Sigma_u^-$	+3.1	+1.1	+0.3	127.6
N_2	$1\,^1\Pi_g$	+4.9	+3.5	+2.8	122.0
N_2	$1\,^1\Delta_u$	+2.7	+1.2	+0.5	126.8
CO	$1\,^1\Pi$	+5.6	+4.2	+3.5	123.5
CO	$1\,^3\Pi$	+2.4	+1.7	+1.4	120.6
HCN	$1\,^1A''$	+2.4	+1.3	+0.8	129.7
C_2	$1\,^1\Pi_u$	+2.2	+1.7	+1.5	131.8
SiO	$1\,^1\Pi$	+12.0	+9.4	+8.4	162.0
SiO	$1\,^3\Delta$	+12.3	+13.6	+13.5	171.5
SO_2	$1\,^3B_1$	+5.8	+3.6	+2.8	149.4
SiF_2	$1\,^1B_1$	+2.7	+2.1	+1.9	160.1
CCl_2	$1\,^1B_1$	−0.3	+0.3	+0.6	165.2
CS_2	$1\,^3A_2$	+0.9	+0.6	+0.5	164.0
HCP	$1\,^1A''$	+2.3	+1.6	+1.4	169.0
BCl	$1\,^1\Pi$	+0.2	+0.9	+1.3	168.9
BCl	$1\,^3\Pi$	+0.5	+1.0	+1.2	169.8
Cl2	$1\,^3\Pi_u$	−9.3	−6.3	−4.7	243.5
CS	$1\,^1\Pi$	+2.5	+2.3	+2.3	157.3
P_2	$1\,^1\Pi_g$	+4.3	+3.5	+3.1	198.9
PN	$1\,^1\Pi$	+4.9	+3.9	+3.5	154.7
AsN	$1\,^1\Pi$	+5.8	+4.3	+3.7	168.7
GaF	$1\,^3\Pi$	+1.5	+1.5	+1.5	174.7
Av. error		2.5	2.1	2.0	
MAE		3.9	3.0	2.6	
Std. Dev.		4.5	3.7	3.3	
Max. Abs.		12.3	13.6	13.5	

Table 3 Errors in adiabatic excitation energies (in eV) for the lowest excited states in some di- and triatomic molecules with respect to the experimental reference valued listed in the right-most column. For diatomic molecules pure electronic excitation energies T_e and for triatomic molecules 0–0 transition energies T_0 are listed. Geometries and vibrational frequencies were determined for each method. For the definition of the average, mean absolute and maximum error and the standard definition see Table 1. The experimental values of the diatomic molecules were taken from ref. 35, the values of the triatomic molecules from the compilation in ref. 20

		CC2	SCS-CC2	SOS-CC2	Exp.
BH	$1\,^1\Pi$	−0.04	+0.02	+0.05	2.87
BF	$1\,^1\Pi$	+0.09	+0.10	+0.10	6.34
BF	$1\,^3\Pi$	−0.17	−0.06	+0.01	3.61
N_2	$1\,^3\Pi_g$	−0.09	+0.14	+0.25	7.39
N_2	$1\,^1\Sigma_u^-$	+0.26	+0.38	+0.43	8.45
N_2	$1\,^1\Pi_g$	−0.19	−0.06	0.00	8.59
N_2	$1\,^1\Delta_u$	+0.43	+0.42	+0.41	8.94
CO	$1\,^1\Pi$	−0.08	+0.03	+0.07	8.07
CO	$1\,^3\Pi$	+0.05	+0.20	+0.28	6.04
HCN	$1\,^1A''$	+0.26	+0.29	+0.30	6.48
C_2	$1\,^1\Pi_u$	+0.34	+0.36	+0.36	1.04
SiO	$1^1\Pi$	−0.50	−0.36	−0.23	5.31
SiO	$1^3\Delta$	−0.34	−0.24	−0.12	4.52
SO_2	1^3B_1	−0.25	−0.00	+0.12	3.19
SiF_2	$1\,^1B_1$	+0.18	+0.22	+0.24	5.34
CCl_2	$1\,^1B_1$	−0.02	+0.05	+0.08	2.14
CS_2	$1\,^3A_2$	+0.06	+0.08	+0.09	3.25
HCP	$1\,^1A''$	+0.20	+0.20	+0.19	4.31
BCl	$1\,^1\Pi$	+0.04	+0.07	+0.08	4.56
BCl	$1\,^3\Pi$	−0.17	−0.05	+0.01	2.50
Cl2	$1\,^3\Pi_u$	+0.15	+0.24	+0.28	2.21
CS	$1\,^1\Pi$	+0.13	+0.18	+0.20	4.82
P_2	$1\,^1\Pi_g$	+0.04	+0.07	+0.09	4.28
PN	$1\,^1\Pi$	−0.02	+0.08	+0.12	4.94
AsN	$1\,^1\Pi$	+0.05	+0.10	+0.12	4.46
GaF	$1\,^3\Pi$	−0.27	−0.20	−0.16	4.10
Av. error		+0.01	+0.09	+0.13	
MAE		0.17	0.16	0.17	
Std. Dev.		0.22	0.18	0.16	
Max. Abs.		0.50	0.42	0.43	

These results demonstrate that the spin-component scaling leads for CC2 to similar systematic improvements for ground state structures and vibrational frequencies as for MP2. It increases in particular the robustness of the second-order approaches with respect to strong correlation effects. As the iterative treatment of the singles amplitudes makes CC2 more sensitive to correlation effects, the improvements obtained by spin-component scaling are in several cases for CC2 even more substantial than for MP2. An exception are, as shown above, covalent bonds between group VI and VII atoms with several lone pairs, for which the spin-component scaling leads to a considerable underestimation of the bond strengths. We note also that this performance of the SCS and SOS versions of MP2 and CC2 does not transfer to weakly bound systems due to a wrong long range behavior of the spin-scaled correlation energy. This might also affect the performance with problems where weak intramolecular bonds or intramolecular dispersion interactions play an important role. A balanced treatment of these effects together with correlation in covalent bonds might be obtained with a range-dependent scaling as proposed by Lochan *et al.* in ref. 34.

V. Electronically excited states

As we have not optimized the spin-component scaling factors or an attenuation factor for the frequency in the denominators of the response matrix, eqn (2.13), one cannot expect a major systematic improvement for excitation energies. We focus in the present study on the question how the spin-component scaling affects the structure and vibrational frequencies of excited states, which is investigated here for the first time. A particular important question is whether an SOS-CC2 model can provide an efficient alternative to TDDFT with hybrid functionals for structure optimizations on large molecules. A major shortcoming of TDDFT with contemporary density functionals is their poor performance for charge-transfer states caused by the incorrect description of the non-local coulomb interaction between donor and acceptor units of the chromophores.

In Table 2 and Fig. 2 we summarized the results for bond lengths in the lowest excited states of some small di- and triatomic molecules. Geometries of excited states of such small molecules are for second-order methods a rather challenging task as—in difference to polyatomic chromophores—here the bonds in the excited state are often elongated to an extent that leads to considerable non-dynamical correlation in the ground state. The performance found for CC2 with this test set is therefore not representative.[20] They constitute, however, a good testing ground for the spin-component scaling as it

Table 4 Errors in caculated 0–0 transition energies (in eV) for organic molecules with typical chromophores, calculated based on DFT geometries and vibrational frequencies. For the definition of the average, mean absolute and maximum error and the standard definition see Table 1; the numbers in parentheses are results evaluated separately for the subsets of $\pi \rightarrow \pi^*$ and $n \rightarrow \pi^*$ excitations, respectively

	Sym.	DFT/TDDFT	CC2	SCS-CC2	SOS-CC2	Exp.	Ref.
$\pi \rightarrow \pi^*$ Excitations							
1,3,5-Hexatriene	1^1B_u	−0.61	−0.21	−0.07	0.01	4.93	36
Benzene	1^1B_{1u}	0.42	0.19	0.01	−0.08	4.72	37
	1^1B_{2u}	−0.18	0.16	0.06	0.01	6.03	38
	1^1E_{1u}	−0.06	−0.01	0.03	0.06	6.87	37
Phenol	$1^1A'$	0.26	0.07	−0.03	−0.08	4.51	39
Benzaldehyde	$1^1A'$	−0.24	0.03	0.06	0.08	5.12	40
Styrene	$2^1A'$	−0.17	0.13	0.20	0.23	4.88	41
	$1^1A'$	0.09	0.29	0.27	0.24	4.31	41
Octatetraene	1^1B_u	−0.68	−0.28	−0.10	−0.01	4.41	42
Naphthalene	1^1B_{2u}	−0.48	−0.14	−0.04	−0.00	4.45	43, 44
	1^1B_{3u}	0.31	0.20	0.11	0.06	3.96	43, 44
Azulene	1^1B_1	0.21	0.09	0.08	0.08	1.77	45
Indole	$1^1A'$	−0.20	−0.00	0.11	0.13	4.54	46
	$1^1A'$	0.35	0.23	0.14	0.10	4.37	46
p-Diethynylbenzene	1^1B_{2u}	0.20	0.18	0.09	0.04	4.25	47
Biphenylene	1^1B_{3u}	0.16	0.04	0.05	0.05	3.55	48[a]
trans-Stilbene	1^1B_u	−0.49	−0.18	−0.06	−0.01	4.00	49
Anthracene	1^1B_{2u}	−0.54	−0.22	−0.05	0.03	3.43	50
Pyrene	1^1B_{2u}	0.08	0.02	−0.05	−0.06	3.44	51[b]
	1^1B_{3u}	−0.39	−0.14	−0.01	0.05	3.81	51[b]
$n \rightarrow \pi^*$ Excitations							
Acetone	1^1A_2	0.09	−0.07	0.06	0.13	3.76	52
Thioacetone	1^1A_2	−0.01	0.02	0.08	0.12	2.33	53
	1^3A_2	−0.30	−0.05	0.08	0.14	2.14	53
Acrolein	$1^1A''$	−0.06	0.07	0.31	0.42	3.21	54
	$1^3A''$	−0.45	−0.10	0.18	0.31	3.01	55
2-Cyclopenten-1-one	$1^1A''$	−0.08	−0.10	0.20	0.34	3.36	56
	$1^3A''$	−0.40	−0.21	0.11	0.26	3.22	57
s-Tetrazine	1^1B_{1u}	−0.29	−0.09	0.13	0.24	2.25	58
Benzaldehyde	$1^1A''$	−0.07	−0.03	0.21	0.32	3.34	59
	$1^3A''$	−0.40	−0.16	0.11	0.25	3.12	59
DMABN	1^1A_2	0.34	−0.08	0.28	0.46	3.95	3, 60, 61[c]
trans-Azobenzene	1^1B_g	−0.67	−0.33	−0.10	0.01	2.60	62[d]
Av. error		−0.13(−0.10/−0.19)	−0.02(0.02/−0.09)	0.08(0.05/0.14)	0.13(0.05/0.25)		
MAE		0.29(0.30/0.26)	0.14(0.16/0.11)	0.14(0.12/0.15)	0.17(0.11/0.13)		
Std. Dev.		0.32(0.34/0.28)	0.17(0.20/0.10)	0.16(0.17/0.11)	0.18(0.17/0.25)		
Max. Abs.		0.68(0.68/0.67)	0.39(0.39/0.33)	0.42(0.42/0.31)	0.46(0.43/0.46)		

[a] In 3-methylpentane. [b] In cyclohexane. [c] Onset of TICT fluorescence in toluene corrected for solvent shift. [d] In hexane.

clearly reveals its effect on the excited state. As the results in Table 2 demonstrate, the spin-component scaling leads in the SCS as well as in the SOS version also for excited states to a very systematic improvement of the bond lengths. The only exceptions where the results obtained with SCS-CC2 deviate more from the experimental results than the CC2 values, are

Table 5 Errors in calculated 0–0 transition energies (in eV) for organic molecules with typical chromophores. Ground and excited state geometries have been optimized for each method and the vibrational frequencies have been taken from the DFT/TDDFT calculation

	Sym.	DFT/TDDFT	CC2	SCS-CC2	SOS-CC2	Exp.	Ref.
$\pi \rightarrow \pi^*$ Excitations							
1,3,5-Hexatriene	1^1B_u	−0.61	−0.21	−0.07	0.01	4.93	36
Phenol	$1^1A'$	0.26	0.06	−0.04	−0.10	4.51	39
Benzaldehyde	$1^1A'$	−0.24	−0.02	0.01	0.02	5.12	40
Naphthalene	1^1B_{2u}	−0.48	−0.13	−0.05	0.01	4.45	43, 44
	1^1B_{3u}	0.31	0.20	0.10	0.05	3.96	43, 44
Octatetraene	1^1B_u	−0.68	−0.29	−0.11	−0.01	4.41	42
Anthracene	1^1B_{2u}	−0.54	−0.22	−0.05	0.03	3.43	50
$n \rightarrow \pi^*$ Excitations							
Acetone	1^1A_2	0.09	−0.19	−0.01	0.07	3.76	52
Thioacetone	1^1A_2	−0.01	−0.01	0.07	0.10	2.33	53
	1^3A_2	−0.30	−0.06	0.07	0.13	2.14	53
Acrolein	$1^1A''$	−0.06	−0.05	0.20	0.31	3.21	54
2-Cyclopenten-1-one	$1^1A''$	−0.08	−0.23	0.11	0.25	3.36	56
	$1^3A''$	−0.40	−0.28	0.07	0.23	3.22	57
Benzaldehyde	$1^1A''$	−0.07	−0.16	0.09	0.21	3.34	59
	$1^3A''$	−0.40	−0.22	0.06	0.20	3.12	59

This journal is © the Owner Societies 2008

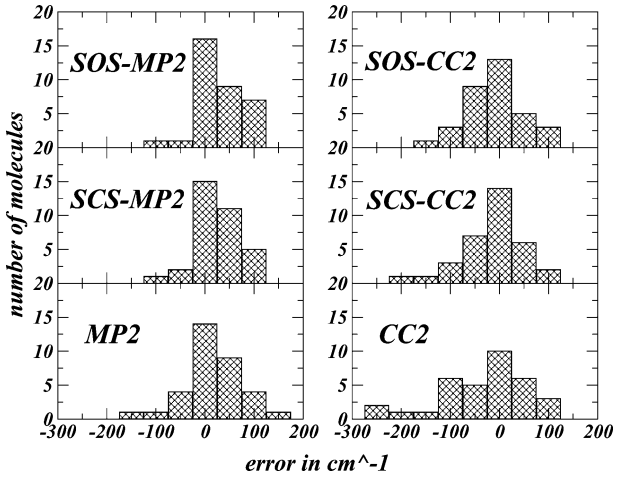


Fig. 1 Error distribution for harmonic vibrational frequencies in the electronic ground state. For technical details of the calculations see text; the experimental reference values were taken from ref. 35.

the $1\,^1\Pi$ and $1\,^3\Pi$ states of BCl and the $1\,^3\Delta$ state of SiO. For the latter molecule, however, already the ground state electronic structure is only poorly described by second-order methods. For SOS-CC2 also the bond lengths for the $1\,^1B_1$ state of CCl_2 is slightly less accurate than that calculated with CC2. The average and the mean absolute errors (MAE) and the standard deviation for the bond distances are significantly reduced by the spin-component scaling. As for the ground state, these trends are also reflected in the results for the harmonic vibrational frequencies as seen in Fig. 3. In all cases where the bond length is improved by the spin-component scaling also the error in the respective vibrational frequency is reduced. For this test set SOS-CC2 performs slightly better than SCS-CC2, but this is probably due to the overemphasis of cases with strong correlation effects in this sample, as will become apparent below. Anyway, the results clearly demonstrate that the spin-component scaled variants of CC2 provide valuable alternatives to CC2 for costly optimization of equilibrium structures of excited states and the calculation of force

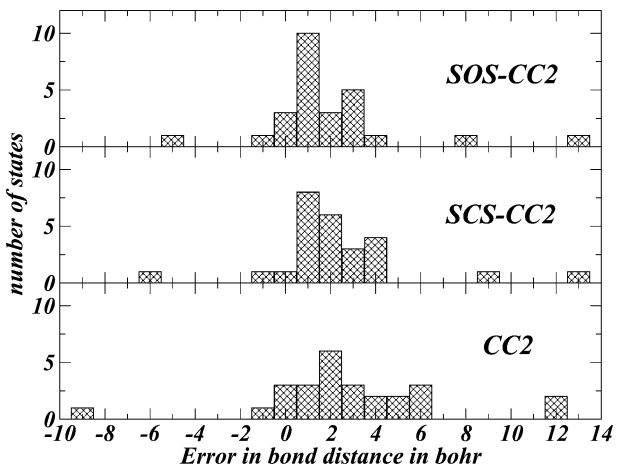


Fig. 2 Error distribution for bond distances in electronic excited states evaluated for the molecules and states listed in Table 2. The experimental values of the diatomic molecules were taken from ref. 35, the values for triatomic molecules are from the compilation in ref. 20.

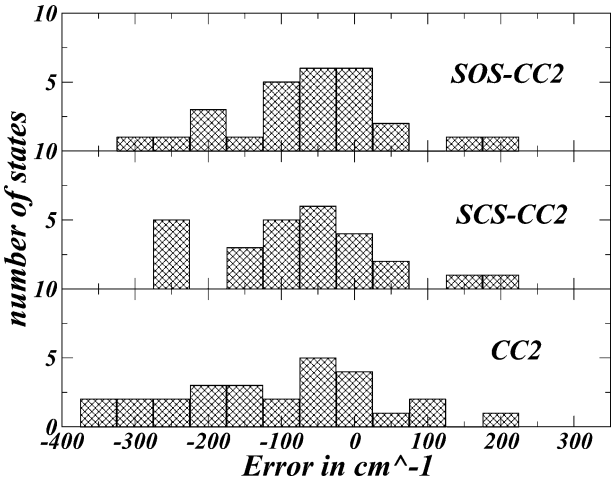


Fig. 3 Error distribution for harmonic vibrational frequencies in electronic excited states evaluated for the di- and triatomic molecules and states listed in Table 2. The experimental values of the diatomic molecules were taken from ref. 35, the values for triatomic molecules are from the compilation in ref. 20.

fields, in particular SOS-CC2, which can be implemented similarly as SOS-MP2 and SOS-CIS(D) with computational costs comparable to those of TDDFT with hybrid functionals.[5–7]

The results for the 0–0 transition energies for this test set are given in Table 3. We find for this sample a slight reduction of the standard deviation and the maximum error for the spin-component scaled versions of CC2, but also a blue shift of the results which is revealed by the increase of the average error from +0.02 eV for CC2 to +0.10 eV for SCS-CC2 and +0.14 eV for SOS-CC2. As a consequence of the blue shift the MAE is for this sample not reduced by the spin-component scaling. It is, however, an encouraging result that without any optimization of the parameters in eqns (2.13) for excitation energies both variants of the spin-component scaling give 0–0 transition energies with a similar accuracy as the original method, but with improved geometries.

In Table 4 we have summarized the results for 0–0 transition energies for a test set of typical $\pi \rightarrow \pi^*$ and $n \rightarrow \pi^*$ excitations in organic molecules which has been used in ref. 3 and 7 to benchmark the performance of spin-component scaled variants of CIS(D). The CC2, SCS-CC2 and SOS-CC2 values given in this table have been obtained using the (TD)DFT geometries and vibrational frequencies and have therefore inherited some errors from the (TD)DFT approach. Nevertheless, these results show that the observations made above for the sample of small inorganic molecules carry over to larger organic molecules which are typically studied with CC2, as seen in Fig. 4. For the whole sample, the spin-component scaling leads to a reduction in the standard deviation, which is, however, accompanied by a blue shift of the results and therefore the mean absolute error is only for SCS-CC2 slightly reduced. As has been observed previously by Grimme and Ugorodina[3] for SCS-CIS(D), $\pi \rightarrow \pi^*$ and $n \rightarrow \pi^*$ excitations respond differently to the spin-component scaling. For the $\pi \rightarrow \pi^*$ excitations there is only a minor blue shift of the average error and the spin-component scaling improves the

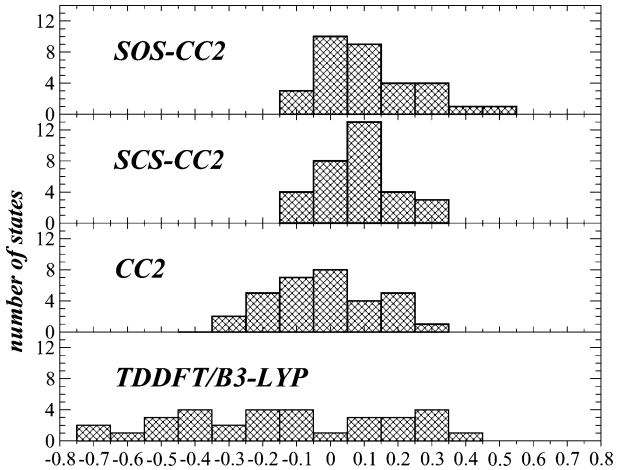


Fig. 4 Distribution of the errors for 0–0 transition energies calculated for the $\pi \rightarrow \pi^*$ and $n \rightarrow \pi^*$ states listed in Table 4, based on equilibrium geometries and vibrational frequencies from (TD)DFT/B3-LYP/TZVP.

results for the excitation energies relatively systematically, which is reflected by a reduction of the MAE and the standard deviation by, respectively, $\sim 1/3$ and almost 50% for this class of excitations. The $n \rightarrow \pi^*$ excitations are, however, substantially blue shifted, in particular with the SOS scaling which shifts the average error from -0.09 eV (CC2) to $+0.25$ eV. This is possibly caused by an overestimation of the correlation in the lone pair from which the excitation occurs. This would be in line with the problems of the spin-component scaled approaches for (ground state) bond distances between atoms with accumulated lone pairs which have been observed in the previous section. Both spin-component scaled versions of CC2 lead for the $n \rightarrow \pi^*$ states in this approach to less accurate results. As shown for SOS-CIS(D) in ref. 7 this can be remedied by attenuating the frequency in the denominators of the response matrix in eqn (2.13) which has not be employed in the present study.

However, the picture changes somewhat when the geometries of the excited states are optimized with the same method as that used to calculate the excitation energies, as seen from the results in Table 5. While the results for the $\pi \rightarrow \pi^*$ excitations change only marginally—which indicates that the DFT geometries for these states are close to those obtained with the CC2 variants—the results for the 0–0 transition energies of the $n \rightarrow \pi^*$ excitations are significantly red shifted compared to the results obtained at the (TD)DFT geometries. The comparatively large differences between the CC2 and the SCS-CC2 and SOS-CC2 results remain, but it is now revealed that (non-scaled) CC2 has a tendency to underestimate 0–0 excitation energies of $n \rightarrow \pi^*$ transitions, which is possibly related to the overestimation of bond distances if strong correlation effects are encountered. This effect is damped by the spin-component scaling in the SCS version which gives the best results for 0–0 transition energies when the geometries are optimized with the same method as used to calculate the energies. The complete neglect of the same-spin component of the double excitation amplitudes leads to an overcorrection with the ground state scaling factor from SOS-MP2 and without optimization of additional parameters for excited states. Nevertheless, the results obtained with this naive SOS-CC2 implementation are already superior to those obtained with B3-LYP.

VI. Summary

In the present study we have shown that the recently suggested spin-component scaled versions of second-order Møller–Plesset perturbation theory (MP2), SCS-MP2 and SOS-MP2, and the perturbative doubles correction to configuration interaction singles, SCS-CIS(D) and SOS-CIS(D), can be generalized in a relatively straightforward way to the approximate coupled-cluster singles-and-doubles model CC2. Both variants of the spin-component scaling have been implemented for CC2 in spin–orbital and spin-free formulations in the parallel RI-CC2 and RI-MP2 program of the TURBOMOLE package for ground and excited state energies and the corresponding analytic gradients. Without any re-optimization of the scaling parameters from SCS-MP2 and SOS-MP2 we obtain already systematic improvements of ground and excited state structures and harmonic vibrational frequencies. The spin-component scaling makes the CC2 model somewhat more robust against strong correlation effects; in particular for systems with triple bonds. In the ground state we find for covalent systems—only for bonds between group VI and VII atoms with accumulated lone pairs—a diminished accuracy with the spin-component scaled variants of CC2. We note, however, that the scaling changes inter- and intramolecular dispersion interaction, as has been discussed for MP2 in ref. 1 and 34. These effects are also found for the spin-component scaled versions of CC2, but we have desisted to discuss examples for this in the present communication.

For 0–0 transition energies the SCS variant leads to a mostly systematic improvement, in particular for $n \rightarrow \pi^*$ excitations in organic molecules, while the SOS variant suffers from a substantial blue shift of excitation energies if used with the scaling factor optimized for MP2 ground state energies and without an attenuation factor for the frequency denominators in the response matrix, so that no improvement is obtained. But if these additional empirical modifications are employed, SOS-CC2 also becomes a competitive approach for excitation energies. As SOS-CC2 can be implemented with computational costs comparable to those of TDDFT with hybrid functionals, it is expected that this approach will become a valuable alternative to TDDFT for large molecules. An implementation of the SOS-CC2 excited state gradients with a fourth-order scaling of the computational costs is currently in progress in our laboratory and will be subject of a forthcoming publication.

Acknowledgements

The present work was supported by the Deutsche Forschungsgemeinschaft (DFG) through project HA2588/2.

References

1. S. Grimme, *J. Chem. Phys.*, 2003, **118**, 9095–9102.

 This journal is © the Owner Societies 2008

2. M. Gerenkamp and S. Grimme, *Chem. Phys. Lett.*, 2004, **392**, 229–235.
3. S. Grimme and E. I. Ugorodina, *Chem. Phys.*, 2004, **305**, 223–230.
4. Y. S. Jung, R. C. Lochan, A. D. Dutoi and M. Head-Gordon, *J. Chem. Phys.*, 2004, **121**, 9793–9802.
5. R. C. Lochan, Y. H. Shao and M. Head-Gordon, *J. Chem. Theory Comput.*, 2007, **3**, 988–1003.
6. Y. S. Jung, Y. H. Shao and M. Head-Gordon, *J. Comput. Chem.*, 2007, **258**, 1953–1964.
7. Y. M. Rhee and M. Head-Gordon, *J. Phys. Chem. A*, 2007, **111**, 5314–5326.
8. J. F. Stanton, J. Gauss, N. Ishikawa and M. Head-Gordon, *J. Chem. Phys.*, 1995, **103**, 4160–4174.
9. A. Köhn and C. Hättig, *J. Am. Chem. Soc.*, 2004, **126**, 7399–7410.
10. C. Hättig, A. Hellweg and A. Köhn, *J. Am. Chem. Soc.*, 2006, **128**, 15672–15682.
11. C. H. Adelia, J. A. Aquino and Hans Lischka, *J. Phys. Chem. A*, 2005, **109**, 3201–3208.
12. E. Fabiano, F. Della Sala, S. Lattante, M. Anni, G. Sotgiu, G. Barbarella, C. Ḧattig, R. Cingolani and G. Gigli, *J. Phys. Chem. B*, 2006, **110**, 18651–18660.
13. W. D. Andrzej, L. Sobolewski and C. Hättig, *J. Phys. Chem. B*, 2006, **110**, 6301–6306.
14. W. D. Andrzej, L. Sobolewski and C. Hättig, *Proc. Natl. Acad. Sci. U. S. A.*, 2005, **102**, 17903–17906.
15. C. Hättig, *J. Chem. Phys.*, 2003, **118**, 7751–7761.
16. T. Helgaker, P. Jørgensen and J. Olsen, in *Molecular Electronic-Structure Theory*, JohnWiley & Sons, New York, 2000, ch. 13, pp. 648–723.
17. C. Hättig, *Adv. Quantum Chem.*, 2005, **50**, 37–60.
18. J. Schirmer, *Phys. Rev. A: At., Mol., Opt. Phys.*, 1981, **26**, 2395–2416.
19. C. Hättig and F. Weigend, *J. Chem. Phys.*, 2000, **113**, 5154–5161.
20. C. Hättig and A. Köhn, *J. Chem. Phys.*, 2002, **119**, 5021–5036.
21. TURBOMOLE, a development of the University of Karlsruhe and Forschungszentrum Karlsruhe GmbH, 1989–2007, TURBOMOLE GmbH, since 2007; available from http://www.turbomole.com.
22. O. Vahtras, J. E. Almlöf and M. W. Feyereisen, *Chem. Phys. Lett.*, 1993, **213**, 514–518.
23. M. W. Feyereisen, G. Fitzgerald and A. Komornicki, *Chem. Phys. Lett.*, 1993, **208**, 359–363.
24. T. H. Dunning, *J. Chem. Phys.*, 1989, **90**, 1007–1023.
25. T. H. Dunning, K. A. Peterson and A. K. Wilson, *J. Chem. Phys.*, 2001, **114**, 9244–9253.
26. F. Weigend, F. Furche and R. Ahlrichs, *J. Chem. Phys.*, 2003, **119**, 12753–12762.
27. A. Schäfer, C. Huber and R. Ahlrichs, *J. Chem. Phys.*, 1994, **100**, 5829.
28. The TURBOMOLE basis set library is available by ftp from ftp://ftp.chemie.uni-karlsruhe.de/pub/basen auxiliary basis sets for RI-MP2 and RI-CC2 calculations are available from ftp://ftp.chemie.uni-karlsruhe.de/pub/cbasen.
29. F. Furche, *J. Chem. Phys.*, 2001, **114**(14), 5982–5992.
30. F. Weigend, A. Köhn and C. Hättig, *J. Chem. Phys.*, 2001, **116**, 3175.
31. C. Hättig, *Phys. Chem. Chem. Phys.*, 2005, **7**, 59–66.
32. C. L. Janssen and I. M. B. Nielsen, *Chem. Phys. Lett.*, 1998, **290**, 423–430.
33. I. M. B. Nielsen and C. L. Janssen, *Chem. Phys. Lett.*, 1999, **310**, 568–576.
34. R. C. Lochan, Y. S. Jung and M. Head-Gordon, *J. Phys. Chem. A*, 2005, **109**, 7593–7605.
35. K. Huber and G. Herzberg, in *NIST Chemistry WebBook, NIST Standard Reference Database Number 69*, ed. P Linstrom and W Mallard, http://webbook.nist.gov, National Institute of Standards and Technology, Gaithersburg MD, 20899, June 2005, chapter Constants of Diatomic Molecules.
36. D. G. Leopold, R. D. Pendley, J. L. Roebber and V. Vaida, *J. Chem. Phys.*, 1984, **81**, 4218.
37. A. Hiraya and K. Shobatake, *J. Chem. Phys.*, 1991, **94**, 7700.
38. O. Christiansen, J. F. Stanton and J. Gauss, *J. Chem. Phys.*, 1997, **108**, 3987.
39. M. J. Watkins, K. Müller-Dethlefs and M. C. R. Cockett, *Phys. Chem. Chem. Phys.*, 2000, **2**, 5528.
40. D. G. Leopold, R. J. Hemley, V. Vaida and J. L. Roebber, *J. Chem. Phys.*, 1981, **75**, 4758.
41. P. Swiderek, M. J. Fraser, M. Michaud and L. Sanche, *J. Chem. Phys.*, 1994, **100**, 70.
42. L. A. Heimbrook, B. E. Kohler and I. J. Levy, *J. Chem. Phys.*, 1984, **81**, 1592.
43. S. M. Beck, D. E. Powers, J. B. Hopkins and R. E. Smalley, *J. Chem. Phys.*, 1980, **73**, 2019.
44. B. Dick and G. Hohlneicher, *Chem. Phys. Lett.*, 1981, **84**, 471.
45. A. A. Ruth, E. K. Kim and A. Hese, *Phys. Chem. Chem. Phys.*, 1999, **1**, 5121.
46. L. Serrano-Andres and B. O. Roos, *J. Am. Chem. Soc.*, 1996, **118**, 185.
47. J. A. Stearns and T. S. Zwier, *J. Phys. Chem. A*, 2003, **107**, 10717.
48. M. E. Beck, R. Rebentisch, G. Hohlneicher, M. P. Fülscher, L. Serrano-Andres and B. O. Roos, *J. Chem. Phys.*, 1997, **107**, 9464.
49. J. A. Syage, W. R. Lambert, P. M. Felker and A. H. Zewail, *Chem. Phys. Lett.*, 1982, **88**, 266.
50. W. R. Lambert, P. M. Felker, J. A. Syage and A. H. Zewail, *J. Chem. Phys.*, 1984, **81**, 2195.
51. P. R. Salvi, P. Foggi and E. Castellucci, *Chem. Phys. Lett.*, 1983, **98**, 206.
52. M. Baba and I. Hanazaki, *Chem. Phys. Lett.*, 1983, **103**, 93.
53. R. H. Judge and D. C. Moule, *Chem. Phys. Lett.*, 1983, **102**, 385.
54. J. Hollas, *Spectrochim. Acta*, 1963, **19**, 1425.
55. A. C. P. Alves, J. Christoffersen and J. M. Hollas, *Mol. Phys.*, 1971, **20**, 625.
56. C. M. Cheatham and J. Laane, *J. Chem. Phys.*, 1991, **94**, 7734.
57. N. R. Pillsbury, J. Choo, J. Laane and S. Drucker, *J. Phys. Chem. A*, 2003, **107**, 10648.
58. E. R. T. Kerstel, M. Becucci, G. Pietraperzia and E. Castellucci, *J. Chem. Phys.*, 1997, **106**, 1318.
59. N. Ohmori, T. Suzuki and M. Ito, *J. Phys. Chem.*, 1988, **92**, 1086.
60. Y. V. Ilichev, W. K̈uhnle and K. A. Zachariasse, *J. Phys. Chem. A*, 1998, **102**, 5670.
61. C. Bulliard, M. Allan, G. Wirtz, E. Haselbach, K. A. Zachariasse, N. Detzer and S. Grimme, *J. Phys. Chem. A*, 1999, **103**, 7766.
62. I. K. Lednev, T. Q. Ye, P. Matousek, M. Towrie, P. Foggi, F. V. R. Neuwahl, S. Umapathy, R. E. Hester and J. N. Moore, *Chem. Phys. Lett.*, 1998, **290**, 68.